Wavelength-selective optical waveguiding of photoluminescence in a thermally annealed Si/SiO_2 superlattice

2004 J. Phys.: Condens. Matter 16 3219

(http://iopscience.iop.org/0953-8984/16/18/022)

INSTITUTE OF PHYSICS PUBLISHING JOURNAL OF PHYSICS: CONDENSED MATTER

J. Phys.: Condens. Matter **16** (2004) 3219–3228 PII: S0953-8984(04)71631-8

Wavelength-selective optical waveguiding of photoluminescence in a thermally annealed Si/SiO_2 superlattice

Leonid Khriachtchev[1,4], **Sergei Novikov**[2], **Jouko Lahtinen**[3] **and Markku Räsänen**[1]

[1] Laboratory of Physical Chemistry, University of Helsinki, PO Box 55, FIN-00014, Finland
[2] Electron Physics Laboratory, Helsinki University of Technology, PO Box 3000, FIN-02015 HUT, Finland
[3] Laboratory of Physics, Helsinki University of Technology, PO Box 1100, FIN-02015 HUT, Finland

E-mail: leonid.khriachtchev@helsinki.fi

Received 10 November 2003
Published 23 April 2004
Online at stacks.iop.org/JPhysCM/16/3219
DOI: 10.1088/0953-8984/16/18/022

Abstract

We investigate the long-distance propagation of broadband photoluminescence (PL) light inside an annealed Si/SiO_2 superlattice (SL) with ∼600 repeats of 1.5 nm Si and 2 nm SiO_2 layers deposited on a silica substrate. The SL material annealed at 1150 °C contains Si nanocrystals with diameters of 3–4 nm as estimated by Raman spectroscopy, and the SL layer was estimated to be overall 1.75 μm thick with an effective refractive index of 1.65. As measured in the conventional transverse detection geometry, the SL material exhibits a broad PL band with a maximum at ∼780 nm (1.6 eV). Our measurements in the waveguiding detection geometry show wavelength selectivity of optical waveguiding by the SL layer. In fact, efficient narrowing of the PL spectrum (down to 16 meV) takes place upon the propagation of the PL light inside the SL layer for wavelengths of 710 and 960 nm. We observed the guiding of PL light by the SL layer to distances above 5 mm, and the propagation losses for the guided light at 710 and 960 nm were estimated to be 6.2 and 4.7 cm^{-1}, respectively. The attenuation of PL light outside the guided wavelengths is much larger (e.g., ∼11 cm^{-1} at 780 nm) demonstrating that Si/SiO_2 SL-based waveguides can be used as optical filters. The transmittance peaks can be tuned by changing the SL layer optical thickness.

[4] Author to whom any correspondence should be addressed.

1. Introduction

The optical and electronic properties of silicon strongly depend on its structure on the nanometre scale [1]. Silicon nanocrystals embedded in an SiO_2 matrix constitute a material of considerable interest for modern photonics. The experimental indications of light amplification (optical gain) in the 1.4–2.0 eV energy region by Si nanocrystals have recently been reported for various Si/SiO_2 materials, giving the promise of a nano-Si laser [2–7]. The optical gain probably occurs in the four-level amplification scheme involving Si=O interface bonds [4–8]. The reports on optical gain have activated studies of propagation of photoluminescence (PL) light in silica containing Si nanocrystals evaluating the reliability of the values obtained for net optical gain [9, 10]. It follows from all those studies that the properties of optical waveguiding are of central importance for the realization of an Si-based active medium. For instance, the wavelength selectivity recently found for waveguiding in silica layers containing Si nanocrystals most probably influences the transmission properties of the active planar waveguide [3, 10].

Among the various deposition methods, Si/SiO_2 nanoscale structures can be prepared using the deposition of repeated ultra-thin Si and SiO_2 layers constituting a so-called Si/SiO_2 superlattice (SL) [6–8, 11–15]. It has been repeatedly reported that the PL of Si/SiO_2 SL samples strongly increases upon thermal annealing above 1000 °C [8, 12, 15]. The thermally enhanced PL around 1.6 eV (780 nm) probably originates from the Si=O covalent bonds localized at the Si/SiO_2 interface of the Si nanostructure [2, 8, 15, 16], in agreement with the 'surface-state model' proposed by Rückschloss *et al* for a relevant Si-based material [17]. The experimental evidence of optical gain has very recently been found for annealed Si/SiO_2 SLs [6, 7] making studies of optical waveguides based on this material important.

We report here the efficient (long-distance) waveguiding of the PL light inside an annealed Si/SiO_2 SL. We study the wavelength selectivity (spectral-filtering effect) of the SL layer and extract its optical parameters (refractive index and losses of optical waveguiding).

2. Experimental details

The Si/SiO_2 SL sample was prepared with a molecular beam deposition system [8, 13–15]. The SiO_2 layers were grown by reactive Si deposition using an RF oxygen plasma cell. The substrate was a 1 mm-thick silica plate. The deposition procedure was previously verified by transmission electron microscopy [13, 15]. In this study, we concentrate on a sample with ∼600 repeats of 1.5 nm Si and 2 nm SiO_2 layers showing good optical waveguiding property. The sample was annealed at 1150 °C in nitrogen atmosphere for 1 h.

The PL measurements were performed using an Ar^+ laser (488 nm, Omnichrome 543-AP) or an He–Ne laser (633 nm, Uniphase 1145P) as the excitation source and a single-stage spectrometer (Acton SpectraPro 500I) equipped with a charge-coupled device camera (Andor InstaSpec IV). In the 'transverse' experimental geometry presented in figure 1(a), the P-polarized laser radiation was focused and directed at ∼45° to the sample surface, and the PL light was detected in the transverse direction [8, 13–15]. In the 'waveguiding' geometry (see figure 1(b)), we used normal incidence (∼0.5 mm in diameter), the collecting objective with 1/8 aperture was focused to the SL edge, and the PL light was detected in the direction parallel to the sample surface [2, 3, 6, 7, 9, 10]. The PL spectra are presented without correction for the spectral sensitivity of the apparatus because relative changes of the spectra are studied here. The Raman spectra were measured in transverse geometry with excitation at 488 nm and resolution of ∼2 cm^{-1}. The UV–visible transmission spectra were obtained with a fibre-optics

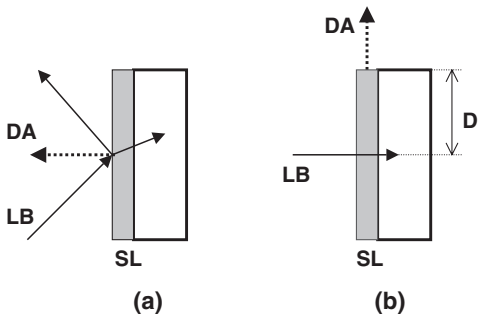

Figure 1. (a) Transverse and (b) waveguiding geometry of photoluminescence detection. LB, DA, and SL denote the incident laser beam, the detection axis, and the superlattice, respectively. D is the distance between the excitation spot and the SL edge.

spectrometer (SD2000, Ocean Optics) and a broadband light source (DH-2000, Top Sensor Systems).

The x-ray photoelectron spectroscopy (XPS) measurements were carried out with an SSX-100 instrument using monochromated Al Kα radiation. The XPS peaks were fitted after Shirley background subtraction using Gaussian lines. In order to probe the elementary composition of the sample bulk, we sputtered the sample material with 1–4 keV Ar^+ providing a sputtering rate up to $\sim$1 nm s^{-1}. Because the ratios between the various suboxide species and the Si network can change during sputtering experiments either due to ion impact or segregation, we did not analyse the chemical shifts during sputtering.

3. Results and discussion

3.1. Sample characterization and PL measured in transverse geometry

The Si crystallization was characterized by Raman spectroscopy and the sample composition was estimated by XPS as described elsewhere [8]. The as-grown material is amorphous, as evidenced by the broad Raman scattering band centred at 470 cm^{-1} (see figure 2(a)). Annealing at 1150 °C promotes crystallization of the Si grains, evidenced by the up-shifting and narrowing Raman band, and a typical crystallite size of 3–4 nm can be estimated using the conventional phonon confinement model [8]. The XPS measurements gave the Si content as $(40 \pm 4)\%$, which was in reasonable agreement with our estimates from the deposition conditions (47%), and no depth dependence of the Si/O concentration was found. No practical impurities (e.g., carbon) were found in the XPS studies.

Figure 2(b) presents optical transmission and reflection spectra of the annealed SL. The spacing of the interference patterns (in cm^{-1}) is connected to the layer thickness via the relation $\Delta\nu = 1/2dn_1$, where n_1 is the effective refractive index of the Si/SiO_2 SL, and the effective optical thickness can hence be extracted. For the present sample, we estimated $\Delta\nu = (1740 \pm 30)$ cm^{-1}. The interference patterns are efficiently suppressed after summarizing the transmission and reflection spectra, which estimates the absorption of the material with the accuracy of scattering [18]. As a result, no distinct absorption band is seen in the spectral range of the PL, in agreement with the recent literature data on relevant Si-based materials [18, 19]. The absorption increases at shorter wavelength (<500 nm), which is attributed to the effect of Si nanostructures [2, 3, 8, 14].

Annealing at 1150 °C enhances the PL intensity typically by an order of magnitude as compared with the as-grown sample [8, 12, 15]. The PL spectra of the annealed sample

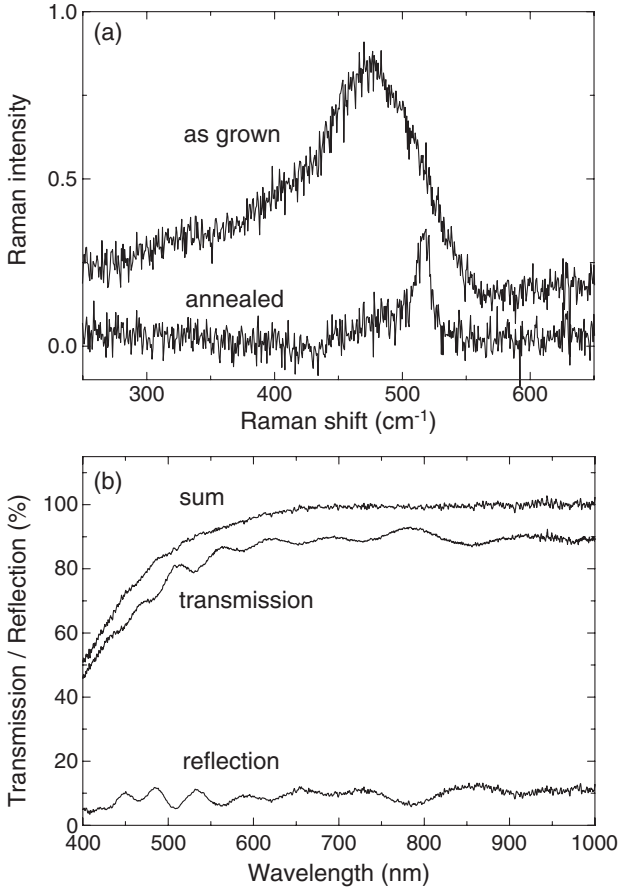

Figure 2. (a) Raman spectra of the as-grown and annealed SL samples. Excitation at 488 nm. (b) Transmission and reflection spectra and the sum of them for the annealed sample. Note the suppression of interference patterns for the summed curve.

measured in transverse geometry appear in figure 3 as smooth profiles with maxima at ∼780 nm (1.6 eV), in agreement with the literature data [8]. The PL light is practically unpolarized. The PL spectra excited at 488 and 633 nm are quite similar, supporting the surface-state model of PL as discussed elsewhere [8, 20]. Furthermore, the PL amplitude is nearly proportional to the excitation power at 488 and 633 nm. This is important to mention because the absorption of the sample material at these two wavelengths differs by about an order of magnitude, as seen in figure 2(b). This experimental fact might mean that the dominating absorbing phase (presumably Si nanostructures) is not directly involved in the emission process. As we have recently discussed [8], the emitting molecule-like phase with Si=O covalent bonds can absorb light without the direct participation of the accommodating Si nanocrystals. As a supporting observation, strong PL at 1.6 eV has been reported from structures with a minor concentration of Si nanocrystals [8, 12].

3.2. Spectral narrowing of PL propagating in a silica layer containing Si nanocrystals

In the waveguiding detection geometry shown in figure 1(b), PL light guided by the SL layer from the excitation spot to the sample edge is detected. This propagation inside the

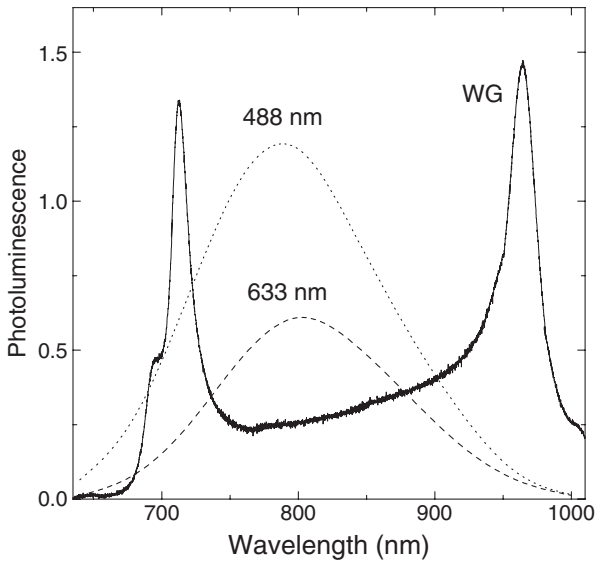

Figure 3. PL spectra of the annealed Si/SiO_2 SL sample. Shown are the spectrum with excitation at 488 nm (40 mW at the sample) measured in transverse geometry (dotted curve), the spectrum with excitation at 633 nm (20 mW at the sample) measured in transverse geometry (dashed curve), and the spectrum with excitation at 633 nm measured in waveguiding geometry ($D = 1$ mm, solid curve). The PL intensities obtained in transverse and waveguiding geometry should not be compared.

SL layer changes the PL spectrum drastically as compared with the original (as-emitted) spectrum detected in transverse geometry. As measured in waveguiding geometry, the PL spectrum exhibits two relatively narrow peaks at about 710 and 960 nm (see the solid curve in figure 3). This experimental data show that the effective refractive index of the SL layer containing Si nanocrystals is somewhat larger than that of the silica substrate providing total internal reflection needed for the waveguiding process [21]. On the other hand, the annealed SL material is rather transparent at the guided wavelengths, allowing long-distance travel of the light (up to 6 mm in these experiments). Most interestingly, the PL spectrum is strongly modified upon waveguiding as seen in figure 3, i.e. the waveguiding efficiency is wavelength-selective. In other words, the PL spectrum detected in waveguiding geometry gives the transmission spectrum of the waveguiding layer with the accuracy of the PL emission profile. The peaks detected in waveguiding geometry (see figure 3) are doublets, and the polarization of the two sub-bands is parallel and orthogonal to the sample, which is characteristic for the H_m and E_m modes of planar waveguides (see also figure 4 for details) [21]. The relative intensities of the H_m and E_m peaks are independent of the incidence polarization. It should also be mentioned that no optical gain is realized under these excitation conditions ($\sim$20 W cm^{-2}), so the spectral narrowing cannot be attributed to stimulated emission. It is important to mention that the detected narrow peaks can be accurately tuned by changing the layer thickness using chemical etching of the SL material with HF. This tunability, illustrated also by the existing literature data [3, 10, 22], means that the observed narrowing is not caused by selective absorption of the material but is introduced by a specific 'cavity effect'. Thus, we can claim that the narrow and polarized spectral peaks are built up upon guiding of the broadband and unpolarized PL light by the silica layer containing Si nanocrystals. This spectral-filtering effect of guided PL light has recently been noticed by us

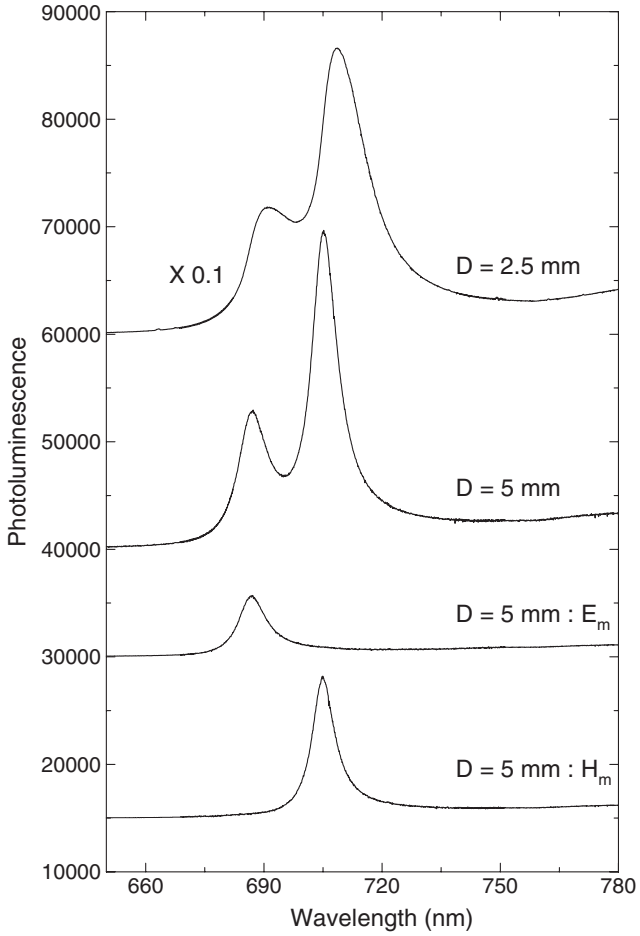

Figure 4. PL spectra measured in waveguiding geometry. Shown are (from top to bottom) the spectrum for $D = 2.5$ mm without polarization analysis, the spectrum for $D = 5$ mm without polarization analysis, the spectrum for $D = 5$ mm in polarization perpendicular to the sample, and the spectrum for $D = 5$ mm in polarization parallel to the sample. The excitation wavelength is 488 nm. Note the multiplication factor for the upper trace.

for annealed Si-rich silica layers [3, 7, 22] and by Valenta *et al* for samples prepared with ion implantation [9, 10].

Now we discuss the mechanism of spectral filtering observed when the broadband PL light propagates long distances inside the silica layer containing Si nanocrystals. As suggested in [22], this phenomenon probably originates from the dependence of attenuation on mode localization. The mode localization is known to be a function of the generalized frequency parameter written for the asymmetrical waveguide in the form

$$V = 2\pi(n_1^2 - n_2^2)^{1/2} d/\lambda \tag{1}$$

where n_1 and n_2 are the refractive indices of the layer and the substrate, respectively, d is the waveguiding layer thickness, and λ is the guided wavelength [21]. The theory of planar optical waveguides shows that the guided modes are the most delocalized at cut-off when $V = (2m + 1)\pi/2$, and the waveguiding attenuation is equal in this case to the bulk loss α_2 of

the substrate. Far above cut-off, the mode becomes localized, and its attenuation approaches the bulk loss α_1 of the layer. When the guiding layer is more absorbing than the substrate ($\alpha_1 n_1 > \alpha_2 n_2$), which is the case here, the more delocalized modes possess smaller attenuation and are mainly supported by the optical waveguide [21]. Thus, minimal losses of the guided modes occur near the mode cut-off when $V = (2m+1)\pi/2$, and equation (1) yields the guided wavelengths.

Based on this model, we estimated the optical properties of the sample. The spectral interval between the two guided spectral peaks was found to be (3670 ± 60) cm^{-1}. By using these data together with $\Delta\nu = 1740$ cm^{-1} and $n_2 = 1.455$, we obtained from equation (1) $n_1 = 1.65$ and $d = 1.75$ μm, and the modes seen in figure 2 corresponded to $m = 3$ (at $\sim$710 nm) and 2 (at $\sim$960 nm). The other possible transmission peaks ($m = 1, 4, \ldots$) do not appear in our spectra because they are well outside the PL spectral region. The obtained refractive index of 1.65 is in good agreement with the value known for as-grown Si/SiO_2 SLs with 1.5 nm-thick Si layers measured with a different method [14], which indirectly supports the present model. A number of factors, however, could limit accuracy of our present estimate. Equation (1) is obtained in the approximation of weakly guiding films [21] when $n_1 - n_2 \ll n_2$ is assumed, but this approximation is quite valid here. Furthermore, the SL is considered in the present model as a single layer with effective (averaged) optical properties, which is also an approximation for SL samples that are generally optically inhomogeneous [14]. In addition, dispersion of the material is neglected here, meaning that only parameters averaged over the spectral interval used can be obtained. It is also understood that the interpretation discussed earlier is rather approximate because additional loss mechanisms (scattering, for example) were neglected. However, for the present consideration, it is mainly important that the periodicity of the wavelength selectivity is controlled by the cut-off condition of the generalized frequency parameter given by equation (1).

3.3. The dependence of guided PL on the propagation distance

Figure 4 presents the spectra detected in waveguiding geometry for two propagation distances D between the excitation spot and the SL layer edge. The detected peaks shift slightly to shorter wavelength and become narrower when D increases. For larger propagation distances, two peaks corresponding to the E_m and H_m modes become well resolved. These spectral components can be very efficiently separated using a polarizer, as presented in the two lower traces in figure 4. It should be mentioned that the exact position and width of the peaks depend to some extent on angular adjustment of the collecting optics, as studied in detail elsewhere [10]. These observations are fully consistent with the narrowing mechanism proposed earlier [22].

The PL peak intensity was measured in waveguiding geometry as a function of the propagation distance, and the result is presented in figure 5(a). It is seen that the dependence is 'anomalous' for small distances of $\sim$1 mm, which feature detection artefacts discussed in particular by Valenta *et al* [9, 10]. However, for longer distances ($\geqslant$2 mm) the dependence is successfully fitted by the evident function:

$$I(D) = I_0 \exp(-k_{WG} D)/D. \tag{2}$$

Fitting of the experimental data with equation (2) allows the propagation loss coefficient, k_{WG}, to be estimated at the guided wavelengths. Apart from the first two data points, presumably mostly influenced by the imperfect detection, the data yielded loss coefficients of (6.2 ± 0.4) and (4.7 ± 0.4) cm^{-1} at 710 and 960 nm, respectively. The ratio of these two PL intensities at 710 and 960 nm should be rather independent of the detection artefacts, and its fitting with the exponential curve gives (1.7 ± 0.3) cm^{-1} for the difference between the loss coefficients at

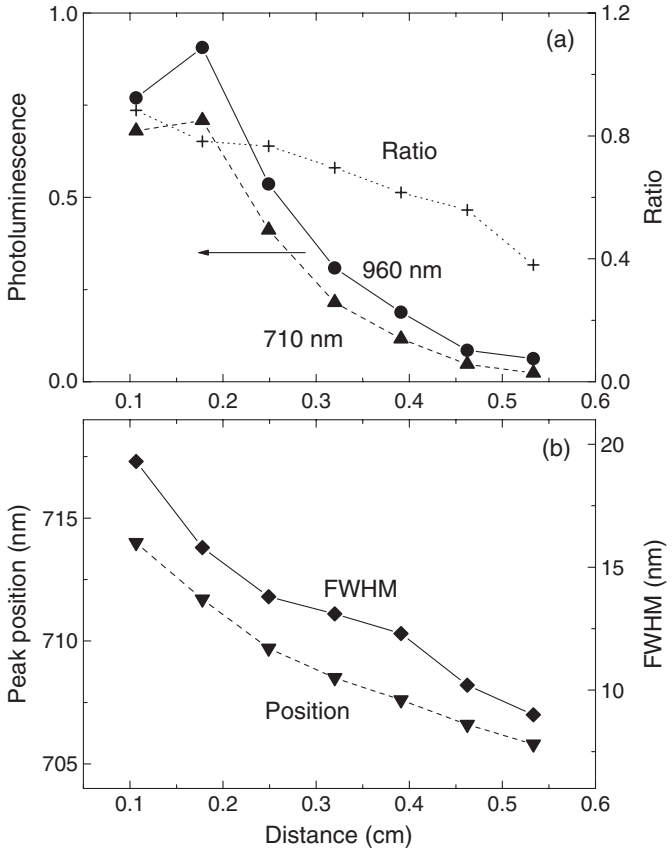

Figure 5. (a) The PL intensity at ∼710 and 960 nm in waveguiding geometry as a function of the distance D between the excitation spot and the SL edge. The data points shown by crosses are the ratios of these two PL intensities. (b) The position of the higher energy PL peak (H_m) and its FWHM as a function of D.

these two wavelengths. This difference value agrees with the 'direct' estimate of losses, which supports the attenuation model described by equation (2). By comparing the PL measured in transverse and waveguiding geometries, we estimated that the propagation loss coefficient at 780 nm is ∼11 cm^{-1}, i.e. it is larger than the loss coefficient at 710 cm^{-1} by ∼6 cm^{-1}. This efficient suppression of PL outside the guided wavelengths characterizes the wavelength selectivity of the waveguiding process.

The propagation losses of light in optical waveguides are contributed to by a number of factors such as material absorption, bulk and surface scattering, diffraction, etc [21]. The contribution of material absorption to the total loss coefficient depends on the mode localization as discussed earlier, and it is minimized for delocalized modes. This means that it is generally difficult to connect the measured propagation loss with the material absorption directly. Most probably the bulk material absorption is smaller than the propagation loss coefficient estimated for non-guided propagation (∼11 cm^{-1} at 780 nm). It should be noted that such weak absorption (extinction coefficient of $\sim 10^{-4}$–10^{-5}) of relevant materials in this spectral region could not be measured by conventional techniques [14, 23]. The propagation loss coefficients obtained in the present study for the guided wavelengths are smaller by a factor of four than

the value at 800 nm obtained by Fauchet and Ruan for the 0.36 μm SL with somewhat thicker Si layers [6]. On the other hand, this attenuation is 3–4 times larger than the corresponding value reported recently by us for the 4.3 μm-thick annealed layer of Si-rich silica [22].

The full widths at half maximum (FWHM) and the peak position of the H_m mode at $\sim$710 nm versus the distance between the excitation spot and the layer edge are given in figure 5(b). The FWHM of about 8 nm ($\sim$16 meV) were obtained for $D = 6$ mm. This narrowing provides an efficient way for spectral control of the transmittance (waveguide-based optical filter) where the transmission spectrum can be tuned by changing the optical thickness. The effect of spectral filtering should be taken into account in possible applications of optical waveguides based on Si nanocrystals, for instance, in a forthcoming nano-Si laser [24].

A number of practical recommendations for measurements of optical gain with the VSL (variable stripe length [2–5, 5–7, 9, 10, 25]) method can be derived from the present results.

(i) The experimental dependence of the detected intensity as a function of the distance described well by equation (2) indicates the essential absence of detection imperfections described in detail elsewhere [9, 10, 25]. This would guarantee a practically linear dependence of the detected intensity on the excitation stripe length without gain for the symmetrical opening of the slit in the VSL method. This linearity is worth checking while studying optical gain.

(ii) We recommend locating the excitation stripe at a possibly longer distance from the layer edge because the guided modes need a distance to be built up, which stabilizes the angular distribution of the radiation emitting from the layer edge [21]. The resolution of the detection optics along the layer should be better than the distance from the edge to prevent the detection of non-guided light.

(iii) The layer optical thickness should be constant, otherwise thickness fluctuations can corrupt the intensity dependences contributing to the propagation attenuation.

(iv) The narrowing of the detected spectrum does not necessarily mean optical gain, but optical filtering can cause it. In addition, the spectral selectivity of optical waveguiding can contribute to the discrepancy between PL and gain profiles reported recently [6, 26].

4. Conclusions

We have investigated the waveguiding properties of an annealed Si/SiO_2 SL with $\sim$600 repeats of 1.5 nm Si and 2 nm SiO_2 layers grown on a silica plate using a molecular beam deposition method. The SL layer was estimated to be effectively 1.75 μm thick with refractive index of 1.65. We observed efficient (long-distance) waveguiding of the PL light by the layer from the excitation area to the sample edge. The optical waveguiding is found to be the most efficient for light at distinct (guided) wavelengths, and these are in the present case $\sim$710 and 960 nm. The losses for the guided modes at $\sim$710 and 960 nm are estimated to be 6.2 and 4.7 cm^{-1}, respectively, which is significantly smaller that the value of 11 cm^{-1} obtained at 780 nm. The transmission peaks can be tuned by changing the optical thickness of the waveguiding layer. Efficient narrowing of the PL spectrum (down to 16 meV) observed in the present study shows, on the one hand, the filtering property of the Si/SiO_2 SL waveguide and requires, on the other hand, precise performance of the waveguide in experiments on optical gain.

Acknowledgment

The Academy of Finland supported this work.

References

[1] Pavesi L 2003 *J. Phys.: Condens. Matter* **15** R1169
[2] Pavesi L, Dal Negro L, Mazzoleni C, Franzo G and Priolo F 2000 *Nature* **408** 440
[3] Khriachtchev L, Räsänen M, Novikov S and Sinkkonen J 2001 *Appl. Phys. Lett.* **79** 1249
[4] Luterova K, Pelant I, Mikulskas I, Tomasiunas R, Muller D, Grob J-J, Rehspringer J-L and Hönerlage B 2002 *J. Appl. Phys.* **91** 2896
[5] Dal Negro L, Cazzanelli M, Daldosso N, Gaburro Z, Pavesi L, Priolo F, Pacifici D, Franzo G and Iacona F 2003 *Physica* E **16** 297
[6] Fauchet P M and Ruan J 2003 *Towards the First Silicon Laser* (*NATO Science Series*) ed L Pavesi, S Gaponenko and L Dal Negro (Dordrecht: Kluwer)
[7] Khriachtchev L and Räsänen M 2003 *Towards the First Silicon Laser* (*NATO Science Series*) ed L Pavesi, S Gaponenko and L Dal Negro (Dordrecht: Kluwer)
[8] Khriachtchev L, Novikov S and Lahtinen J 2002 *J. Appl. Phys.* **92** 5856
[9] Valenta J, Pelant I and Linnros J 2002 *Appl. Phys. Lett.* **81** 1396
[10] Valenta J, Pelant I, Luterova K, Tomasiunas R, Cheylan S, Elliman R G, Linnros J and Hönerlage B 2003 *Appl. Phys. Lett.* **82** 955
[11] Lu Z H, Lockwood D J and Baribeau J-M 1995 *Nature* **378** 258
[12] Sullivan B T, Lockwood D J, Labbe H J and Lu Z-H 1996 *Appl. Phys. Lett.* **69** 3149
[13] Khriachtchev L, Räsänen M, Novikov S, Kilpelä O and Sinkkonen J 1999 *J. Appl. Phys.* **86** 5601
[14] Khriachtchev L, Novikov S and Kilpelä O 2000 *J. Appl. Phys.* **87** 7805
[15] Khriachtchev L, Kilpelä O, Karirinne S, Keränen J and Lepistö T 2001 *Appl. Phys. Lett.* **78** 323
[16] Wolkin M V, Jorne J, Fauchet P M, Allan G and Delerue C 1999 *Phys. Rev. Lett.* **82** 197
[17] Rückschloss M, Landkammer B and Veprek S 1993 *Appl. Phys. Lett.* **63** 1474
[18] Khriachtchev L 2002 *Appl. Phys. Lett.* **81** 1357
[19] Elliman R G, Lederer M J and Luther-Davies B 2002 *Appl. Phys. Lett.* **80** 1325
[20] Gole J L, Dudel F P, Grantier D and Dixon D A 1997 *Phys. Rev.* B **56** 2137
[21] Unger H G 1977 *Planar Optical Waveguides and Fibers* (Oxford: Clarendon)
[22] Khriachtchev L, Räsänen M and Novikov S 2003 *Appl. Phys. Lett.* **83** 3018
[23] Inokuma T, Wakayama Y, Muramoto T, Aoki R, Kurata Y and Hasegawa S 1998 *J. Appl. Phys.* **83** 2228
[24] Jaiswal S L, Simpson J T, Withrow S P, White C W and Norris P M 2003 *Appl. Phys.* A **77** 57
[25] Valenta J, Luterova K, Tomasiunas R, Dohnalova K, Hönerlage B and Pelant I 2003 *Towards the First Silicon Laser* (*NATO Science Series*) ed L Pavesi, S Gaponenko and L Dal Negro (Dordrecht: Kluwer)
[26] Dal Negro L, Cazzanelli M, Pavesi L, Ossisini S, Pacifici D, Franzo G, Priolo F and Iacona F 2003 *Appl. Phys. Lett.* **82** 4636